Spontaneous subpicosecond pulse formation with pulse repetition rate of 80 GHz in a diode-pumped Nd:$SrGdGa_3O_7$ disordered crystal laser

Y. F. Chen,[1,*] H. C. Liang,[1] J. C. Tung,[1] K. W. Su,[1] Y. Y. Zhang,[2] H. J. Zhang,[2] H. H. Yu,[2] and J. Y. Wang[2]

[1]*Department of Electrophysics, National Chiao Tung University, Hsinchu 30010, Taiwan*

[2]*State Key Laboratory of Crystal Materials and Institute of Crystal Materials, Shandong University, Jinan 250100, China*

**Corresponding author: yfchen@cc.nctu.edu.tw*

Received November 2, 2011; revised December 20, 2011; accepted December 20, 2011;
posted December 20, 2011 (Doc. ID 157449); published February 6, 2012

We explore the operation of spontaneous mode locking in a diode-pumped Nd:$SrGdGa_3O_7$ disordered crystal laser. The first- and second-order autocorrelations are simultaneously performed to evaluate the temporal characteristics. An 80 GHz pulse train with a pulse duration as short as 616 fs is observed. The maximum output power is 415 mW at a pump power of 6.1 W.

OCIS Codes: 140.3380, 140.4050, 140.6810.

Since disordered laser crystals have the properties of broad absorption and emission spectra and high thermal conductivity, they have recently attracted a great deal of attention for achieving powerful ultrashort pulse lasers. The Nd:ABC_3O_7 crystals are a class of disordered laser gain media [1–3], where A = Ca, Sr, Ba; B = La, Gd; and C = Ga, Al. In addition to the Nd:$SrLaGa_3O_7$ and Nd:$BaLaGa_3O_7$ crystals, the Nd:$SrGdGa_3O_7$ (Nd:SGGM) is another kind of Nd:ABC_3O_7 crystal [4–6]. In the Nd:SGGM crystal, Nd^{3+} ions substitute for Sr^{2+} and Gd^{3+} ions that are distributed randomly in a 1∶1 ratio [7–9], producing a disordered structure and large inhomogeneous spectral broadening. This feature is not only beneficial to diode pumping but also for the production of ultrashort pulses.

For ideal mode locking, all modes of the whole spectrum of a multimode laser have equally separated frequency differences and time-independent constant amplitudes to lead to a train of bandwidth-limited short pulses [10]. The occurrence of spontaneous mode locking is an intriguing phenomenon observed in a laser system without any saturable absorber. This phenomenon has been observed on different types of lasers, including He–Ne [11], ruby [12], Nd-doped crystal [13], argon ion [14], fiber [15], and semiconductor [16–18] laser systems. Realistically, the spontaneous mode locking belongs to a nonideally mode-locked operation. The time dependence of a multimode laser at a point in the cavity can be given by

$$E(t) = \mathrm{Re}\left\{e^{-i(\omega_c - N\Omega/2)t}\sum_{n=1}^{N} a_n(t)e^{-i[n\Omega t+\varphi_n(t)]}\right\}, \quad (1)$$

where ω_c is the central frequency, Ω is the frequency spacing of adjacent longitudinal modes, N is the total number of lasing modes, and $a_n(t)$ and $\varphi_n(t)$ are the real amplitude and phase of the nth mode. Weber and Dändliker [19] explored the time-dependent output intensity of a nonideally mode-locked laser by considering the influence of statistical phase variations in the modes of a multimode laser. They found that, as long as the phase variations is not completely random, the output intensity of a multimode laser can maintain a train with the pulse duration the same as that of ideally mode-locked pulses.

Figure 1 shows three numerical examples of the instantaneous intensity for 10 modes with equal amplitude and with the phases randomly distributed in the interval $(-\varphi, +\varphi)$, where the results include $\varphi = 0$, $\varphi = \pi/6$, and $\varphi = \pi/3$. It can be seen that the influence of the phase variations in a multimode laser is only to introduce a fluctuating background to the ideally mode-locked intensity. The phase variations in diode-pumped lasers are expected to be considerably less than those in lamp pumped counterparts because the thermal effect is significantly reduced.

In this Letter we explore the performance of the spontaneous mode locking in a diode-pumped Nd:SGGM disordered crystal laser. We control the separation between the gain medium and the end mirror to reach the tenth-order harmonic mode-locked operation with repetition rate up to 80 GHz. Under the absorbed pump power of 6.1 W, an average output power of 415 mW was obtained, corresponding to optical efficiency of 6.8% and slope efficiency of 8.1%. The pulse width was measured to be 616 fs at the output power of 400 mW. This pulse duration

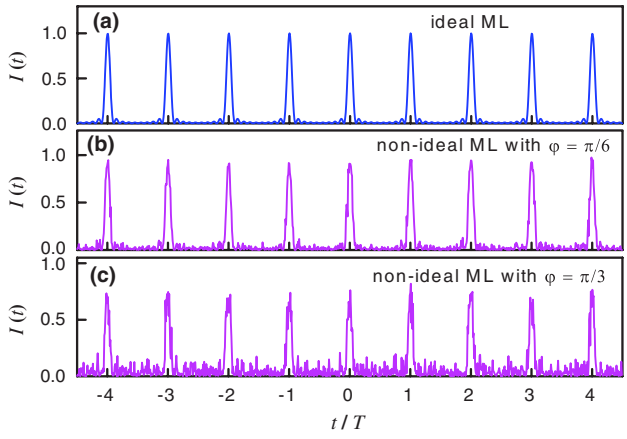

Fig. 1. (Color online) Numerical examples with Eq. (1) for 10 modes with equal amplitude and with the phases randomly distributed in the interval $(-\varphi, +\varphi)$, where (a) $\varphi = 0$, (b) $\varphi = \pi/6$, and (c) $\varphi = \pi/3$.

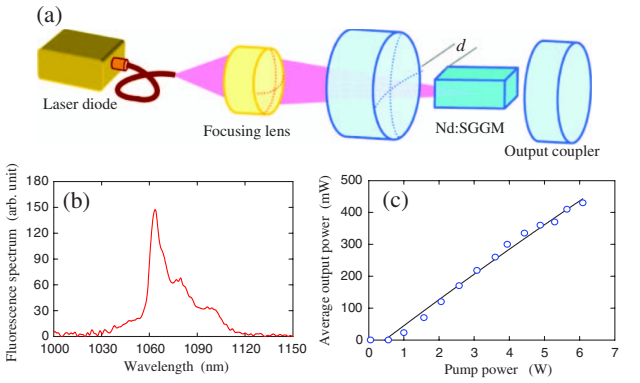

Fig. 2. (Color online) (a) Experimental setup of a spontaneous mode-locking laser system. (b) Fluorescence spectrum for the ${}^4F_{3/2} \rightarrow {}^4I_{11/2}$ at room temperature. (c) Experimental result for the average output power versus the incident pump power.

is the shortest ever obtained in spontaneous mode-locked Nd-doped crystal lasers so far as we know.

Figure 2(a) depicts the cavity configuration, which is a linear concave–plano resonator. The gain medium is c-cut 1.3 at. % Nd:SGGM crystal with dimensions of $3\,\text{mm} \times 3\,\text{mm} \times 6\,\text{mm}$. The level lifetime of the excited state was measured to be approximately 284 μs [9]. Both end surfaces of the laser crystal were polished with no coating. Figure 2(b) shows the fluorescence spectrum for the ${}^4F_{3/2} \rightarrow {}^4I_{11/2}$ at room temperature. Luminescence bandwidth can be seen to be nearly 24 nm. The laser crystal was wrapped with indium foil and mounted in a water-cooled copper holder. The water temperature was maintained at around 20 °C to ensure stable laser output. The input mirror was a 50 mm radius-of-curvature concave mirror with antireflection coating at 808 nm on the entrance face and with high-reflectance coating at 1060 nm (>99.8%) and high-transmittance coating at 808 nm on the second surface. A flat wedged output coupler with a reflection coefficient of 97.5% at 1060 nm was used in the experiment. The pump source was a 7 W 808 nm fiber-coupled laser diode with core diameter of 200 μm and NA of 0.20. A focusing lens with 25 mm focal length and 87% coupling efficiency was used to reimage the pump beam into the laser crystal. The average pump diameter was approximately 200 μm. The optical cavity length was set to be approximately $L = 19$ mm, corresponding to a free spectral range of 8 GHz. Becker *et al.* [20] found that the etalon effect formed by the separation between the laser crystal and the input mirror, d, could play an important role in modulating the optical spectrum of a mode-locked laser. In the present experiment, we found that varying the separable d in the range of 1–5 mm could lead to harmonic mode locking with different orders and the frequency was usually between 80 and 180 GHz. With the etalon effect, the separation d was experimentally found to be related to the expression L/N, where the integer N corresponded to the Nth harmonic mode locking. We also observed that the separation $d = 1.9$ mm favored the tenth-order harmonic mode locking. Figure 2(c) depicts the experimental result for the average output power versus incident pump power. The average output power was 415 mW at an incident pump power of 6.1 W.

The temporal output was systematically analyzed by taking first- and second-order autocorrelations. Note that no peaks were observed in the real-time trace and rf spectrum up to 10 GHz bandwidth limit of the instrument. Perhaps this is why the phenomenon of self-mode-locking in several tens of gigahertz has not been discovered earlier. No signs of Q-switched mode locking were observed in either autocorrelation or the rf spectrum. The lack of peaks in the rf spectrum and the peak spacing in the optical spectrum provide excellent evidence for harmonic mode locking. The first-order autocorrelation trace was measured using a Michelson interferometer (Advantest, Q8347). The autocorrelation interferometer is also capable of performing optical spectral analysis by Fourier transforming the first-order field autocorrelation. In comparison with the conventional second-order autocorrelation measurement, the high sensitivity and dynamic range of the Michelson interferometer [21] enable us to assess the optimal cavity adjustment for spontaneous mode-locked operation. Figure 3(a) shows the experimental first-order autocorrelation trace under the tuning condition of obtaining maximum power output. The pulse separation can be seen to be approximately 12.5 ps. It corresponds to a repetition rate of 80 GHz, i.e., the tenth-order harmonic mode locking. The temporal amplitude also displays a modulation frequency equal to second-order harmonic frequency. This modulation amplitude is mainly due to the supermode competition activated by the longitudinal spatial hole burning effects [20,22]. Two sets of interleaved longitudinal modes can be clearly observed from the optical spectrum shown in Fig. 3(b). We experimentally found that the tenth-order harmonic mode locking could be considerably improved by finely tuning the crystal/mirror separation d. Figures 4(a) and (b) show, respectively, the experimental first-order autocorrelation trace and optical spectrum under the optimum tenth-order harmonic mode locking at

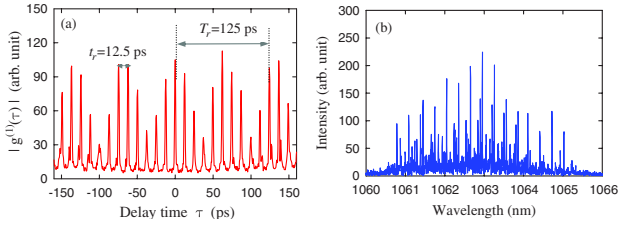

Fig. 3. (Color online) (a) Experimental first-order autocorrelation trace under the tuning condition of obtaining maximum power output. (b) Optical spectrum centered near 1063 nm.

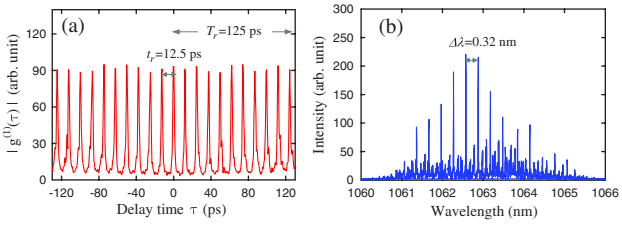

Fig. 4. (Color online) (a) Experimental first-order autocorrelation trace and optical spectrum under the tuning condition of obtaining optimum harmonic mode locking at the output power of 400 mW. (b) Optical spectrum centered near 1062.5 nm.

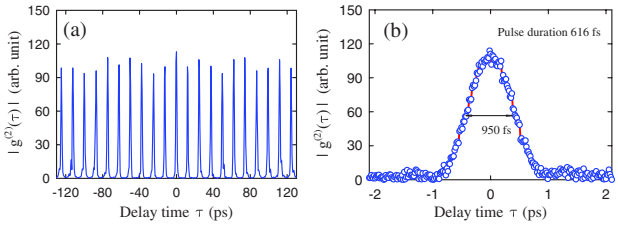

Fig. 5. (Color online) (a) Second-order autocorrelation trace corresponding to the result shown in Fig. 4(a). (b) Higher-resolution autocorrelation of one pulse.

the output power of 400 mW. The major mode spacing can be seen to be approximately 0.32 nm. This value is consistent with the pulse repetition rate of 80 GHz. There are many minor lasing longitudinal modes appearing in the optical spectrum. We did not further improve the mode-locked performance. The unwanted lasing modes can be effectively suppressed by using a Fabry–Perot etalon [22].

The second-order autocorrelation traces were also performed with a commercial autocorrelator (APE pulse check, Angewandte Physic & Elektronik GmbH). Figure 5(a) shows the second-order autocorrelation trace corresponding to the experimental result shown in Fig. 4(a). On the whole, both the pulse separation and the temporal structure can be seen to be almost the same as the results shown in Fig. 4(a) for the first-order autocorrelation trace. This remarkable resemblance indicates that the overall optical spectrum has a nearly constant phase [23]. As shown in Fig. 5(b), the FWHM width of the central peak in the second-order autocorrelation trace is approximately 950 fs. If the temporal intensity is assumed to be a sech^2 profile, the pulse duration can be deduced to be as short as 616 fs. From Fig. 4(b), the optical spectral width can be seen to be approximately 2.1 nm with the central wavelength at 1062.5 nm. As a result, the time–bandwidth product of the mode-locked pulse can be found to be 0.33, which is quite close to the Fourier-limited value. The subpicosecond pulse train with very high repetition rate is attractive especially for communications via time multiplexing.

In conclusion, we have demonstrated what we believe to be the the first experimental observation of spontaneous mode locking in a diode-pumped Nd:SGGM disordered crystal laser. The separation between the gain medium and the end mirror was delicately tuned to reach the tenth-order harmonic mode locking with repetition rate up to 80 GHz. The pulse width was measured to be as short as 616 fs at the output power of 400 mW.

The authors acknowledge the National Science Council of Taiwan for their financial support of this research under contract NSC 100-2628-M-009-001-MY3.

References

1. T. T. Basiev, N. A. Es'kov, A. Ya. Karasik, V. V. Osiko, A. A. Sobol, S. N. Ushakov, and M. Helbig, Opt. Lett. **17**, 201 (1992).
2. J. Petit, P. Goldner, and B. Viana, Opt. Lett. **30**, 1345 (2005).
3. A. García-Cortés, J. M. Cano-Torres, M. D. Serrano, C. Cascales, C. Zaldo, S. Rivier, X. Mateos, U. Griebner, and V. Petrov, IEEE J. Quantum Electron. **43**, 758 (2007).
4. A. V. Terentiev, P. V. Prokoshin, K. V. Yumashev, V. P. Mikhailov, W. Ryba-Romanowski, S. Golab, and W. Pisarski, Appl. Phys. Lett. **67**, 2442 (1995).
5. M. A. Scott, D. L. Russell, B. Henderson, T. P. J. Han, and H. G. Gallagher, J. Cryst. Growth **183**, 366 (1998).
6. W. Ryba-Romanowski, S. Gołąb, G. Dominiak-Dzik, W. A. Pisarski, M. Berkowski, and J. Fink-Finowicki, Spectrochim. Acta A **54**, 2071 (1998).
7. V. Kushawaha and L. Major, Appl. Phys. B **57**, 447 (1993).
8. V. Kushawaha and Y. Chen, Appl. Phys. B **60**, 67 (1995).
9. Y. Y. Zhang, H. J. Zhang, H. H. Yu, J. Y. Wang, W. L. Gao, M. Xu, S. Q. Sun, M. H. Jiang, and R. I. Boughton, J. Appl. Phys. **108**, 063534 (2010).
10. A. E. Siegman, *Lasers* (University Science, 1986).
11. M. H. Crowell, IEEE J. Quantum Electron. **1**, 12 (1965).
12. H. Statz and C. L. Tang, J. Appl. Phys. **36**, 3923 (1965).
13. H. C. Liang, R. C. C. Chen, Y. J. Huang, K. W. Su, and Y. F. Chen, Opt. Express **16**, 21149 (2008).
14. O. L. Gaddy and E. M. Schaefer, Appl. Phys. Lett. **9**, 281 (1966).
15. P. Glas, M. Naumann, A. Schirrmacher, L. Däweritz, and R. Hey, Opt. Commun. **161**, 345 (1999).
16. R. Paiella, F. Capasso, C. Gmachl, D. L. Sivco, J. N. Baillargeon, A. L. Hutchinson, A. Y. Cho, and H. C. Liu, Science **290**, 1739 (2000).
17. J. Renaudier, B. Lavigne, F. Lelarge, M. Jourdran, B. Dagens, O. Legouezigou, P. Gallion, and G. H. Duan, Electron. Lett. **41**, 1007 (2005).
18. C. Gosset, K. Merghem, A. Martinez, G. Moreau, G. Patriarche, G. Aubin, A. Ramdane, J. Landreau, and F. Lelarge, Appl. Phys. Lett. **88**, 241105 (2006).
19. H. P. Weber and R. Dändliker, J. Eur. Opt. Soc. Rapid Pub. **5**, 10050s (2010).
20. M. F. Becker, D. J. Kuizenga, and A. E. Siegman, IEEE J. Quantum Electron. **8**, 687 (1972).
21. M. De Maziere, A. Bouwen, and D. Schoemaker, J. Opt. Soc. Am. B **6**, 2370 (1989).
22. R. Wessel, R. Ricken, K. Rochhausen, H. Suche, and W. Sohler, IEEE J. Quantum Electron. **36**, 394 (2000).
23. A. M. Weiner, *Ultrafast Optics* (Wiley, 2009).